Chapter 8: Channel and Pipe Flow (Chap. 7 Bernard)

Part 2: Pipe Flow

$R_e \sim 2000$ transition turbulence.

$$R_e = \frac{U_m D}{\nu} \qquad U_m = \frac{Q}{A}$$

Fully developed flow: $\underline{\overline{U}} = \left(\overline{U}(r), 0,0\right) \rightarrow$ averaged streamwise momentum equation:

$$0 = -\frac{\partial \overline{p}}{\partial x} + \frac{1}{r}\frac{d}{dr}\left(\mu r \frac{d\overline{U}}{dr} - \rho r \overline{u v_r}\right) \quad (1)$$

Where r is the outward radial coordinate, i.e., $r = 0$ at the center of the pipe and $r = R_0$ at the wall. Introduce wall coordinate:

$$y \equiv R_0 - r$$

Such that:

$$\overline{U}^*(y) = \overline{U}(R_0 - y)$$

However, the $*$ symbol will be dropped.

The wall shear stress:

$$\tau_w = \mu \frac{d\overline{U}}{dy}(0)$$

Which also defines $R_\tau = \frac{U_\tau D}{\nu}$ where $U_\tau = \sqrt{\frac{\tau_w}{\rho}}$ = friction velocity.

Integrating Eq. (1) over the pipe cross-section yields

$$0 = \int_0^{R_0} \int_0^{2\pi} -\frac{\partial \overline{p}}{\partial x} + \frac{1}{r}\frac{d}{dr}\left(\mu r \frac{d\overline{U}}{dr} - \rho r \overline{u v_r}\right) r dr d\theta$$

$$0 = -\pi R_0^2 \frac{\partial \overline{p}}{\partial x} - 2\pi R_0 \tau_w$$

$$-\pi R_0^2 \frac{\partial \overline{p}}{\partial x} = 2\pi R_0 \tau_w \quad (2)$$

Since

$$\frac{d\overline{U}}{dr}(R_0) = -\frac{d\overline{U}}{dy}(0)$$

And

$$\overline{v_r}(0) = \overline{u v_r}(0) = \overline{u v_r}(R_0) = 0$$

Eq. (2) shows that $\frac{\partial \overline{p}}{\partial x} = f(\tau_w)$.

The volumetric flow rate:

$$Q = 2\pi \int_0^{R_0} \overline{U}(r) dr$$

can be determined once $\overline{U}(r)$ is known, which determines the averaged velocity U_m = Q/A where A=πR_0^2 and defines the Reynolds number

$$R_e = \frac{U_m D}{\nu}$$

Define friction factor for pipe flow f as:

$$f = \frac{\Delta \overline{p}}{\Delta x} \frac{2D}{\rho U_m^2} = 8 \frac{R_\tau^2}{R_e^2} = \frac{8\tau_w}{\rho U_m^2} \quad (3)$$

The Moody diagram can be used to find values of $f(Re)$.

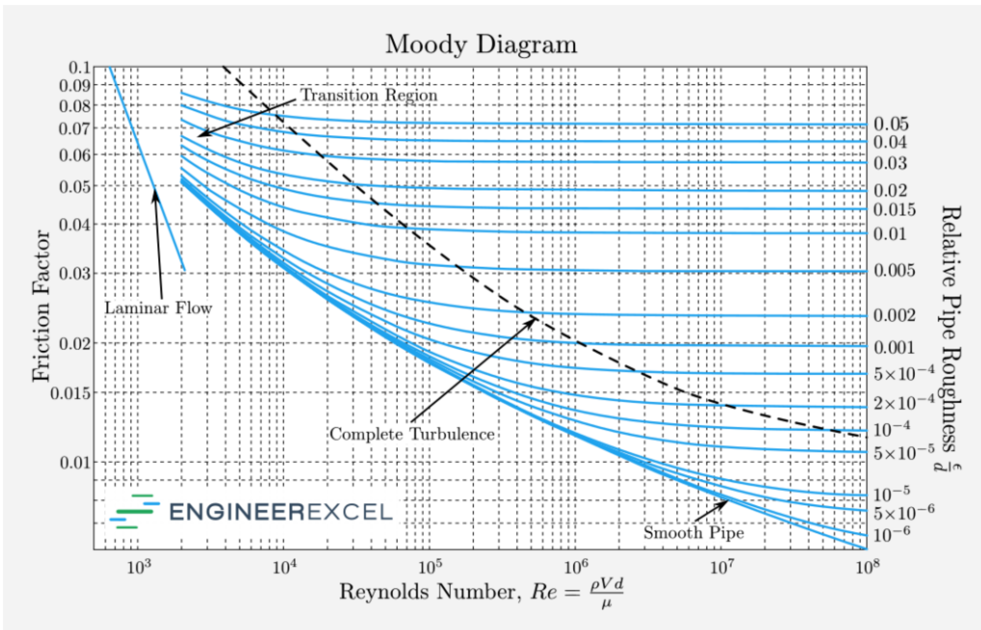

Current analysis presumes that the pipe is smooth. For engineering applications, it is necessary to consider $f(Re, \frac{\varepsilon}{d})$, where $\frac{\varepsilon}{d}$ represents the relative pipe roughness.

Alternatively explicit formulas are available for smooth and rough pipes, e.g.:

For $R_e < 10^5$, the Blasius smooth pipe friction law

$$f = 0.266 R_e^{-1/4}$$

And substituting this into Eq. (3) gives a relationship between R_τ and R_e

$$R_\tau = 0.182 R_e^{7/8}$$

Previous channel flow analysis neglected outer layer, which should be included for pipe and especially BL flows.

In viscous sublayer ($y^+ < 5$):

$$\overline{U}^+ = y^+$$

And log law valid for intermediate layer of pipe flow: $\overline{U}^+ = \frac{1}{\kappa} ln y^+$+B.

For high Re pipe flow, central core mean velocity cannot be scaled using viscosity, so similarity is achieved using the velocity defect law:

$$\frac{\overline{U}_{cl} - \overline{U}(y)}{U_\tau} = g(\xi)$$

Where $\overline{U}_{cl}$ = mean centerline velocity and $\xi \equiv y/R_0$ is a similarity variable. In practice, this equation is found to work also in most of the intermediate region.

If velocity defect law applies in overlap region, then:

$$f(y^+) = \overline{U}^+ = \frac{\overline{U}_{cl}}{U_\tau} - g(\xi) \quad (4)$$

Differentiating Eq. (4) with respect to y gives

$$\frac{df}{dy^+}(y^+)\frac{U_\tau}{\nu} = -\frac{dg}{d\xi}(\xi)\frac{1}{R_0} \qquad \boxed{y^+ = \frac{U_\tau y}{\nu}}$$

And multiplying both sides of the equation by y gives:

$$y^+ \frac{df}{dy^+}(y^+) = -\xi \frac{dg}{d\xi}(\xi) \quad (5)$$

LHS only f(y^+) and RHS only f(ξ); thus, both sides must be equal and constant. Setting the constant to be $1/k$:

$$y^+ \frac{df}{dy^+}(y^+) = \frac{1}{k}$$

Integration gives the log law:

$$\overline{U}^+ = k^{-1} \log y^+ + B$$

i.e., using velocity defect law in intermediate layer recovers log-law.

New high Re data shows $k = 0.42$, $B = 5.6$ for $600 \leq y^+ \leq 0.12 R_0^+$ vs. historical 0.41 and 5.2.

The details of the velocity defect law for outer flow will be analyzed for BL flow.

In the region beyond the viscous sublayer, up to $y^+ \sim 300$, a power law gives:

$$\overline{U}^+ = 8.48(y^+)^{0.142}$$

For $5 < y^+ < 300$.

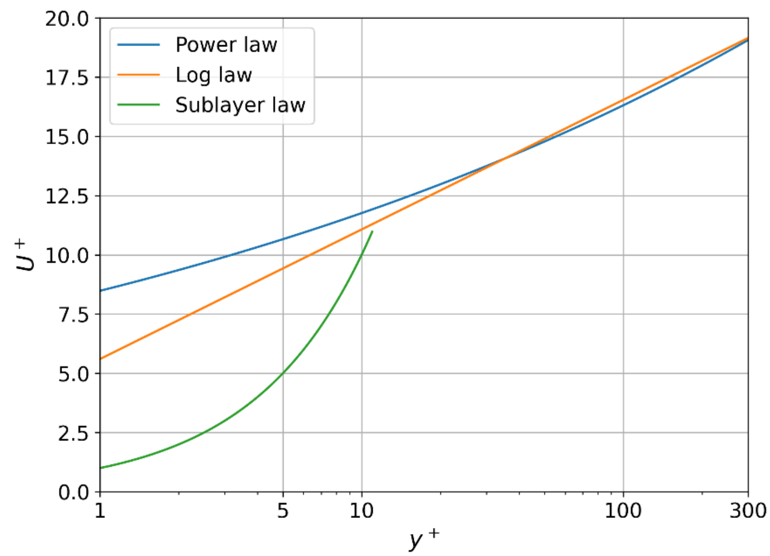

When compared with previously defined composite sub-layer, blending layer, and logarithmic-overlap formula

$$U^+ = y^+ - e^{-\kappa B}\left[e^{\kappa u^+} - 1 - \kappa U^+ - \frac{(\kappa U^+)^2}{2} - \frac{(\kappa U^+)^3}{6}\right]$$

Shows its limitations.

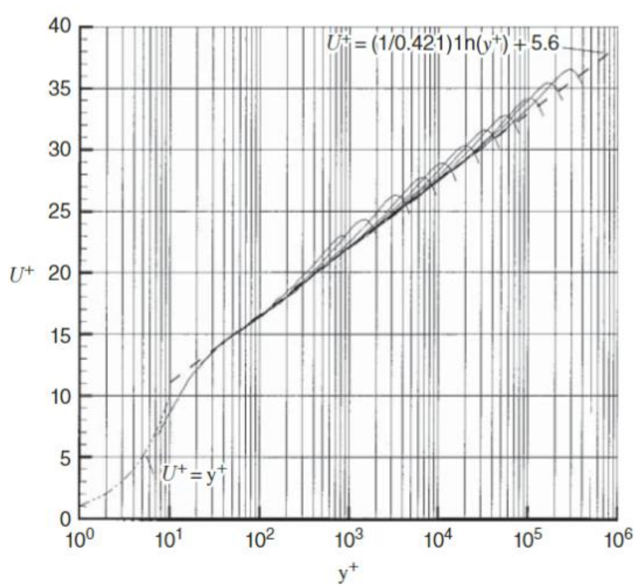

Figure 7.18 Mean velocity profiles in pipe flow [6] showing the collective approach to a log law. The curves are for Reynolds numbers between $R_e = 31 \times 10^3$ and $R_e = 18 \times 10^6$. Reprinted with permission of Cambridge University Press.

Power Law

Early studies showed that power laws can represent flow behavior over the entire pipe cross-section:

$$\frac{\overline{U}}{U_{cl}} = \left(\frac{y}{R_0}\right)^{1/n}$$

Where n increases with Re, shows good fit with data, but cannot provide τ_w.

Taking a derivative of the power law gives:

$$\frac{d\overline{U}}{dy} = \frac{U_{cl}}{n}\left(\frac{y}{R_0}\right)^{\frac{1}{n}-1}$$

Where experimental fits show that $n \sim 6 - 10$, such that $\frac{1}{n} - 1 \sim -(0.85 - 0.9)$. Therefore, e.g., for n = 10:

$$\frac{d\overline{U}}{dy}(0) \sim \frac{U_{cl}}{n}\left(\frac{R_0}{y}\right)^{0.9}$$

Showing that the shear stress approaches ∞ as $y \to 0$.

Linear-log plots of power law show good fit to the data for range of n:

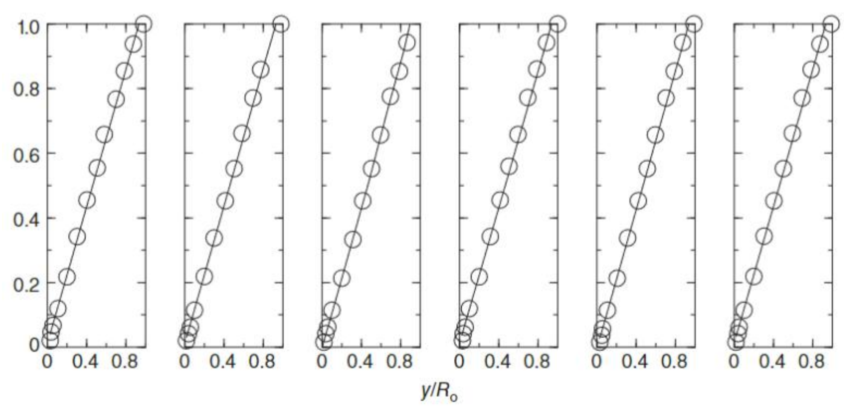

Figure 7.19 Plots of $(\overline{U}/\overline{U}_{max})^{1/n}$ in pipe flow for empirically fitted exponents, n. From left to right n ~~1/n~~ = 6.0, 6.6, 7.0, 8.8, 10.0, and 10.0, and the Reynolds numbers are 4×10^3, 2.3×10^4, 1.1×10^5, 1.1×10^6, 2×10^6, and 3.2×10^6. From [25], p. 563.

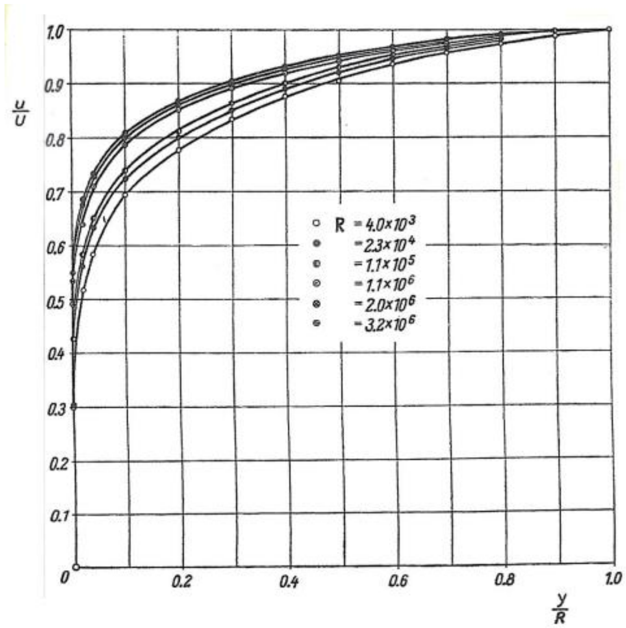

Fig. 20.2. Velocity distribution in smooth pipes for varying Reynolds number, after Nikuradse [45]

Subsequently, power laws were generalized to include not only inner law variables (y, τ_w, ν, ρ) but also outer law variable R_0, i.e., $d\overline{U}/dy = f(y, \tau_w, \nu, \rho, R_0)$ for the intermediate layer to include dependence on ν and R_0, i.e., generalization of the log law approach, but in this case not independent of Re (partial similarity).

Dimensional analysis gives:

$$\frac{d\overline{U}}{dy} = \frac{U_\tau}{y} f(y^+, R_\tau) \quad (6)$$

But since R_τ is related to R_e, Eq. (6) can be rewritten as:

$$\frac{d\overline{U}}{dy} = \frac{U_\tau}{y} f(y^+, R_e) \quad (7)$$

If $f =$ constant, log law is implied, alternatively if f obeys a power law:

$$f(y^+, R_e) = \beta^*(R_e)(y^+)^{\alpha(R_e)} \quad (8)$$

For large y^+ and R_e.

Both $\overline{U}^+$ and f will follow power laws after integration of Eq. (7) using (8).

$$d\overline{U} = \frac{U_\tau}{y}\beta^*(R_e)(y^+)^{\alpha(R_e)}dy$$

$$d\overline{U}^+ = \beta^*(y^+)^{\alpha-1}dy^+$$

$$\int_{\overline{U}^+(0)}^{\overline{U}^+(y^+)} d\overline{U}^+ = \beta^* \int_0^{y^+} (y^+)^{\alpha-1}dy^+$$

$$\boxed{\begin{gathered} y^+ = \frac{U_\tau y}{\nu} \\ dy^+ = \frac{U_\tau}{\nu}dy \\ \overline{U}^+ = \frac{\overline{U}}{U_\tau} \end{gathered}}$$

Applying BC at the wall gives:

$$\overline{U}^+(y^+) = \frac{\beta^*}{\alpha}(y^+)^\alpha$$

$$\overline{U}^+(y^+) = \beta(R_e)(y^+)^{\alpha(R_e)} \quad (9)$$

Where β is defined from α and β^* after the integration, i.e., β=$\beta^*/\ \alpha.$

To determine a form of $\alpha(R_e)$, consider behavior of Eq. (9) as ν→ 0. If $\frac{\partial\overline{p}}{\partial x}$ is constant, τ_w remains constant as ν→ 0, and so does U_τ, as per Eq. (2).

Since $\overline{U}$ is bounded, $\overline{U}^+$ is bounded, so LHS of Eq. (9) is bounded as ν→ 0.

Consequently, RHS must be bounded as $y^+ \to \infty$ and $R_e \to \infty$.

Noting the identity

$$(y^+)^{\alpha(R_e)} = e^{\alpha(R_e)\log y^+}$$

Eq. (9) can be rewritten as:

$$\overline{U}^+(y^+) = \beta(R_e)e^{\alpha(R_e)\log y^+}$$

$\alpha(R_e)$ is assumed of the form:

$$\alpha(R_e) = \frac{\alpha_1}{\log R_e}$$

Such that:

$$\overline{U}^+(y^+) = \beta(R_e)(y^+)^{\frac{\alpha_1}{\log R_e}}$$

and gives good agreement with experiments. It is assumed that $\beta(R_e)$ shows the same dependence on R_e as α:

$$\beta(R_e) = \beta_0 + \frac{\beta_1}{\log R_e}$$

Where β_0 and β_1 are constants.

It is then derived that:

$$\overline{U}^+(y^+) = \left(\beta_0 + \frac{\beta_1}{\log R_e}\right)(y^+)^{\frac{\alpha_1}{\log R_e}} \quad (10)$$

Where the appearance of R_e in the form of its logarithm means that if R_e is replaced by $\gamma R_e \rightarrow \log \gamma R_e = \log \gamma + \log R_e$, which converges to $\log R_e$ as $R_e \rightarrow \infty$.

α_1 and β_1 should have universal form and together with β_0 are determined by empirical fit, comparing with EFD data.

For $4 \times 10^3 \leq R_e \leq 3.24 \times 10^6$: $\alpha_1 = 1.5$, $\beta_0 = 0.578$, and $\beta_1 = 2.5$.

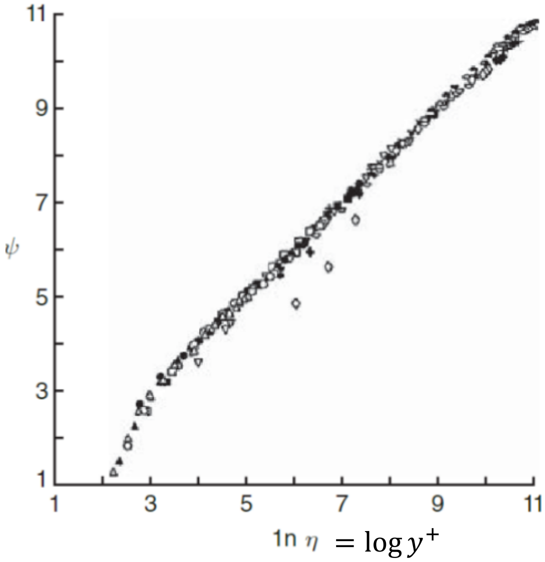

Figure 7.20 ψ vs. $\log y^+$ where $\eta \equiv y^+$ in this figure. Data are taken from 16 different Reynolds numbers from 4×10^3 to 3.24×10^6 measured in [29]. From [31]. Reprinted with permission from ASME International.

$$\psi \equiv \frac{\log R_e}{\alpha_1} \log \left(\frac{\overline{U}^+}{\beta_0 + \frac{\beta_1}{\log R_e}} \right)$$

From Eq. (10):

$$\frac{\overline{U}^+}{\beta(R_e)} = (y^+)^{\frac{\alpha_1}{\log R_e}} = a$$

$$\log a = \frac{\alpha_1}{\log R_e} \log y^+ \rightarrow \log y^+ = \frac{\log R_e}{\alpha_1} \log a = \psi$$

i.e., Eq. (10) is equivalent to $\psi = \log y^+$.

Since the power law is meant to cover larger region of the pipe than the log law, it can be used to explain large y^+ departure from log law.

Pope 7.3.4

In the overlap region $(\nu/U_\tau \ll y \ll \delta)$ two velocities profiles are possible, i.e., the log law:

$$u^+ = \frac{1}{k}\log y^+ + B$$

And the power law:

$$u^+ = C(y^+)^\alpha$$

The coefficients k, B, α, and C can be $f(R_e)$. If that's not the case, the laws are said to be universal.

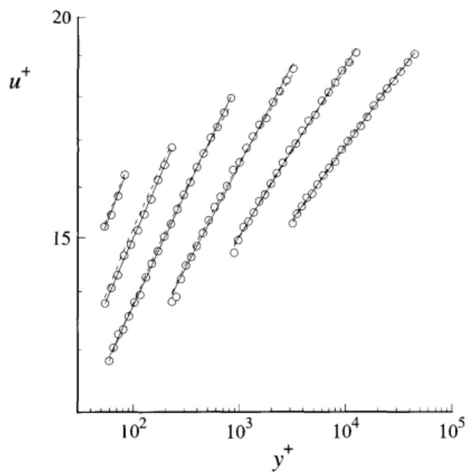

Fig. 7.31. A log–log plot of mean velocity profiles in turbulent pipe flow at six Reynolds number (from left to right: Re $\approx 32 \times 10^3$, 99×10^3, 409×10^3, 1.79×10^6, 7.71×10^6, and 29.9×10^6). The scale for u^+ pertains to the lowest Reynolds number: subsequent profiles are shifted down successively by a factor of 1.1. The range shown is the overlap region, $50\delta_\nu < y < 0.1\,R$. Symbols, experimental data of Zagarola and Smits (1997); dashed lines, log law with $\kappa = 0.436$ and $B = 6.13$; solid lines, power law (Eq. (7.157)) with the power α determined by the best fit to the data.

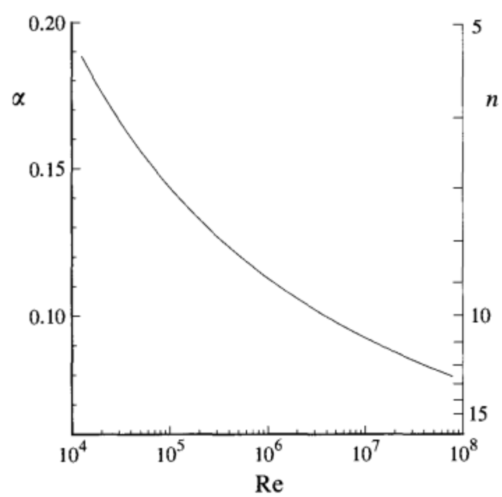

Fig. 7.32. The exponent $\alpha = 1/n$ (Eq. (7.158)) in the power-law relationship $u^+ = C(y^+)^\alpha = C(y^+)^{1/n}$ for pipe flow as a function of the Reynolds number.

It is clear that α decreases significantly with R_e. An empirical formula is given by:

$$\alpha = \frac{1.085}{\log R_e} + \frac{6.535}{(\log R_e)^2}$$

Vs Bernard $\alpha = \frac{\alpha_1}{\log R_e} = \frac{1.5}{\log R_e}$

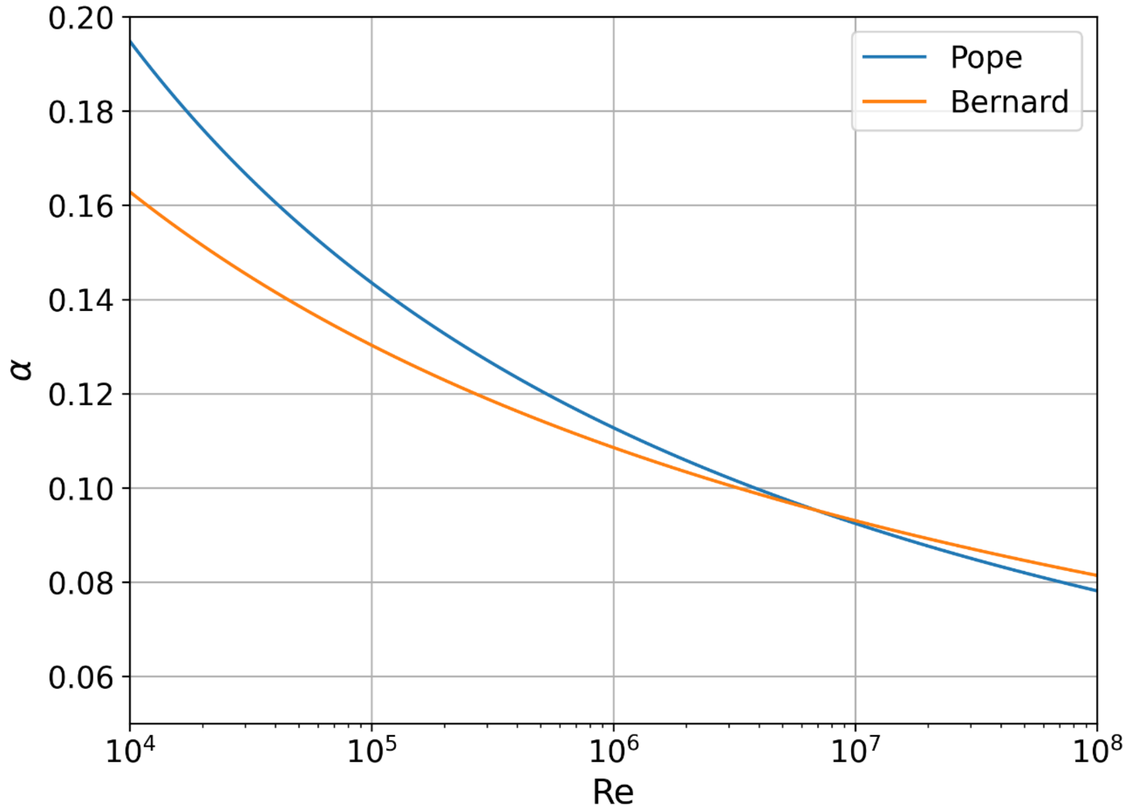

Streamwise normal RS $\overline{u^2}$ for high Re data shows 2nd peak in addition to peak at $y^+ = 15$, but reason for this is still under discussion.

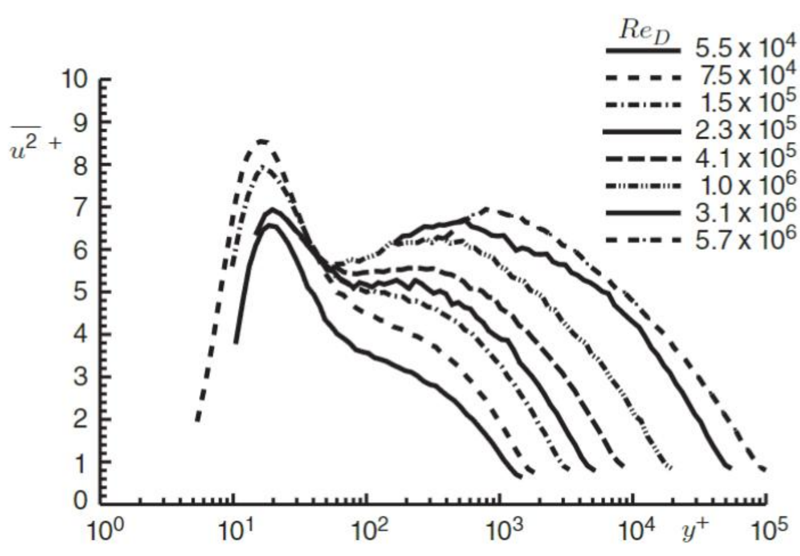

Figure 7.21 Streamwise velocity variance at high Reynolds numbers in pipe flow [32]. Reprinted with permission of Cambridge University Press.

Appendix

Roughness

k = roughness height

$k^+ = \frac{k u^*}{\nu}$

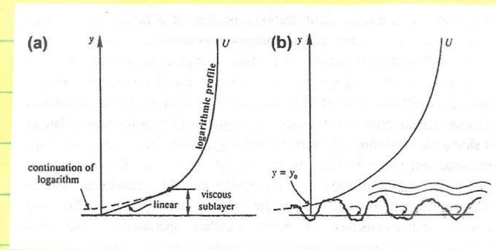

$k^+ < 4$ hydraulically smooth

$4 < k^+ < 60$ transitional roughness $f(Re)$

$k^+ > 0$ fully rough $\neq f(Re)$

$$U/u^* = \frac{1}{\kappa} \ln y^+ + B + \frac{2\Pi}{\kappa} W(y/\delta) - \Delta U^+$$

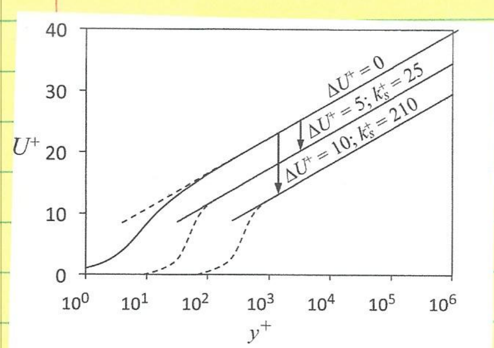

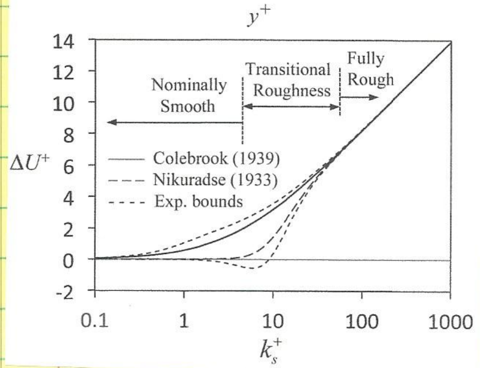

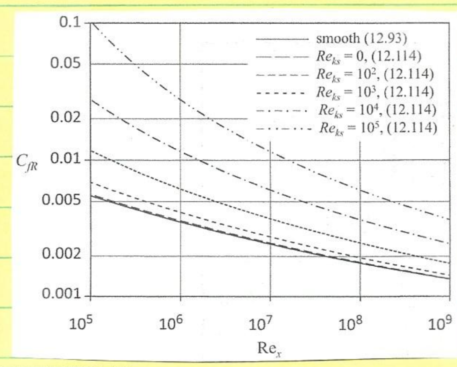

FIGURE 12.25 Rough surface skin friction coefficient, C_{fR}, for a zero-pressure-gradient flat-plate turbulent boundary layer vs. Re_x, the Reynolds number based on downstream distance. The solid curve corresponds to (12.93) evaluated using log-law constants $\kappa = 0.39$ and $B = 4.3$ (as recommended by Marusic et al., 2013). The dashed and dash-dot curves come from implicit evaluation of (12.114) for equivalent-sand-grain roughness-height Reynolds numbers of $Re_{ks} = 0, 10^2, 10^3, 10^4$, and 10^5. The C_{fR} values produced by (12.114) agree within engineering accuracy (± 5% or so) with prior rough-plate results.